acta physica slovaca 42 (1992). No. 1, 9–22

NON-STATIONARY COMPUTER MODEL OF THE ASYMPTOTIC REGION OF AN ELECTRIC ARC GAS HEATER

JENIŠTA, J.[1]), SEDLÁČEK, Z.[1]), Prague

A method for the numerical solution is presented of the non-stationary energy balance equation in the asymptotic region of an electric arc gas heater with axial gas supply which makes it possible to distinguish between stable and unstable solutions and to examine in detail the transient phenomena occurring during the formation of the stationary state.

I. INTRODUCTION

The present paper is concerned with the computer model of the asymptotic region of the discharge channel of an electric arc gas heater with cylindrical geometry (the so-called fully developed electric arc). The system of equations of magnetohydrodynamics describing this region is reduced to the equation of energy balance.

A number of methods exists for the solution of the stationary variant of this equation (the so-called Elenbaas–Heller equation). The simplest of these is the so-called channel model [2] based on the approximation of the radial profile of the electric conductivity by a piece-wise constant function which, in the elementary case, may consist of two sections: constant conductivity at the axis and zero conductivity at the wall. Other methods use approximation by piece-wise linear functions, expansion into Bessel functions etc. [1]. The most accurate methods use procedures which are unavoidable for two-dimensional (r, z) models: the stationary state is achieved from a suitably chosen initial distribution of physical quantities by an iterative process over a succession of intermediate states. In the present paper we solve the real transient process during the formation of the stationary state. This makes it possible to study the non-stationary behaviour of an arc gas greater such as the process of arc ignition dynamics or the time response of an electric arc

[1]) Institute of Plasma Physics, Czechoslovak Academy of Sciences, pod Vodárenskou věží 4, 182 11 PRAGUE 8, CSFR

as an element of the electrical circuit with the source of the electromotoric force, resistance, capacity and inductivity. This is important for the investigation of the stability of operation of real arc gas heaters.

II. BASIC EQUATIONS

The dynamics of electric arc plasma is described by the set of equations of magnetohydrodynamics which include the equation of continuity, the equation of motion (the Navier–Stokes equation with the Lorentz force), the equation of energy balance, the Maxwell equations, the generalized Ohm's law and the state equation of a perfect gas.

We assume a cylindrical coordinate system r, φ, z and the boundary-layer approximation (radial gradients are much greater than axial gradients), which simplifies significantly the basic set of equations. Under these assumptions the set of equations of magnetohydrodynamics may be written as follows [2]:

Continuity equation:

$$\frac{\partial \varrho}{\partial t} + \frac{1}{r}\frac{\partial}{\partial r}(r\varrho v) + \frac{\partial}{\partial z}(\varrho u) = 0. \qquad (1)$$

Momentum equation:

$$\frac{\varrho w^2}{r} = \frac{\partial p}{\partial r} + j_z B, \qquad (2)$$

$$\varrho\frac{\partial w}{\partial t} + \frac{\varrho v}{r}\frac{\partial}{\partial r}(rw) + \varrho u\frac{\partial w}{\partial z} = \frac{1}{r}\frac{\partial}{\partial r}\left[\eta r^3 \frac{\partial}{\partial r}\left(\frac{w}{r}\right)\right], \qquad (3)$$

$$\varrho\frac{\partial u}{\partial t} + \varrho v\frac{\partial u}{\partial r} + \varrho u\frac{\partial u}{\partial z} = -\frac{\partial p}{\partial z} + j_r B + \frac{1}{r}\frac{\partial}{\partial r}\left(\eta r\frac{\partial u}{\partial r}\right). \qquad (4)$$

Energy balance equation:

$$\varrho\frac{\partial H}{\partial t} + \varrho v\frac{\partial H}{\partial r} + \varrho u\frac{\partial H}{\partial z} - \frac{\partial p}{\partial t} = \sigma E_z^2 + \frac{1}{r}\frac{\partial}{\partial r}\left(r\frac{\lambda}{c_p}\frac{\partial H}{\partial r}\right) + \frac{1}{r}\frac{\partial}{\partial r}\left[r\left(\eta - \frac{\lambda}{c_p}\right)\frac{\partial}{\partial r}\left(\frac{V^2}{2}\right) - \eta w^2\right] - \Psi. \qquad (5)$$

Maxwell's equations:

$$j_z = \frac{1}{r}\frac{\partial}{\partial r}(rH_\varphi), \qquad (6)$$

$$E_z = E(z,t). \qquad (7)$$

Ohm's law:

$$j_z = \sigma E_z. \qquad (8)$$

The equation of state:

$$p = \frac{R_0 \varrho T}{M} \qquad (9)$$

Here the following notation is used: r, φ, z— cylindrical coordinates, v, w, u—velocity components in a cylindrical coordinate system, p—hydrodynamic pressure, j_z, j_r—z and r components of a current density $\boldsymbol{j}$, E_z—z component of the electric field strength $\boldsymbol{E}$, B—magnetic induction, H_φ—φ component of the magnetic field strength $\boldsymbol{H}$, σ—electric conductivity, λ—thermal conductivity, η—dynamic viscosity, ϱ—mass density, c_p—specific heat at constant pressure, Ψ—radiative energy emitted per unit volume and unit time, h—specific enthalpy, $H = h + V^2/2$—the "total" enthalpy; $V^2 = u^2 + w^2$, R_0—universal gas constant, M—molecular mass.

It is further necessary to specify the relevant boundary and initial conditions. The material and thermodynamic functions σ, λ, η, ϱ, c_p, Ψ, H are strongly non-linear functions of temperature and are weakly dependent on pressure.

The above set of equations in usually regarded as the most general mathematical model of the electric arc plasma with rotational symmetry ($\partial/\partial\varphi = 0$). It has not been solved numerically in its most general form as yet, only particular simplified models exist.

III. THE COMPUTER MODEL

Our aim was to set up a simple computer model which would enable us to study the dynamic properties of the electric arc plasma and which would, in principle, be suitable for possible future extensions to two- or three- dimensional models.

The computational model is derived from the above set of magnetohydrodynamic equations under these additional assumptions:

1. The model describes the asymptotic region of a cylindrically symmetric electric arc discharge (the fully developed electric arc) inside a circular metallic tube of radius R, kept at a fixed temperature T_R (stabilization by a cold wall). This means that all physical quantities are independent of the axial coordinate z.
2. The tangential (w) and radial (v) components of velocity are neglibible.
3. The gas flow is characterized by a small Mach number ($M < 0.3$). The kinetic energy carried by the gas is then negligible in comparison with the heat energy and it is possible to solve the equation of energy balance separately from the momentum equation.

Our task is thus to solve the equation

$$\frac{\partial T}{\partial t} = \frac{1}{\varrho c_p}\left[\sigma E_z^2 + \frac{1}{Pr}\frac{1}{Re}\frac{1}{r}\frac{\partial}{\partial r}\left(r\lambda\frac{\partial T}{\partial r}\right) - \Psi\right] \qquad (10)$$

with the boundary conditions

$$T(R,t) = T_R \quad \text{(fixed wall temperature)} \tag{11}$$

$$\left.\frac{\partial T}{\partial r}\right|_{r=0} = 0 \quad \text{(the condition of axial symmetry)} \tag{12}$$

and the initial condition

$$T(r, t=0) = T_0(r). \tag{13}$$

Here the dimensionless quantities

$$t = \frac{t' u_0}{L_0}, \quad r = \frac{r'}{L_0}, \quad T = \frac{T'}{T_0},$$
$$\varrho = \frac{\varrho'}{\varrho_0}, \quad c_p = \frac{c_p'}{c_{p0}}, \quad \sigma = \frac{\sigma'}{\sigma_0} \tag{14}$$
$$E_z = \frac{E_z'}{E_0}, \quad \lambda = \frac{\lambda'}{\lambda_0}, \quad \Psi = \frac{\Psi'}{\Psi_0}$$

were introduced. In numerical calculations, the results of which are presented in the next section, the following values of the normalization constants have been used: $u_0 = 100\ \mathrm{ms^{-1}}$, $L_0 = R = 0.01$ m, $T_0 = 1000$ K, $\varrho_0 = 0.01\ \mathrm{kgm^{-3}}$, $c_{p0} = 10\,000\ \mathrm{JK^{-1}kg^{-1}}$, $E_0 = 1000\ \mathrm{Vm^{-1}}$, $\lambda_0 = 1\ \mathrm{WK^{-1}m^{-1}}$. The normalization constants σ_0, Ψ_0 are related to the remaining ones by the formulas

$$\sigma_0 = \frac{\varrho_0 c_{p0} u_0 T_0}{E_0^2 L_0} = 10^3 S, \quad \Psi_0 = \frac{\varrho_0 c_{p0} u_0 T_0}{L_0} = 10^9 \mathrm{Wm^{-3}} \tag{15}$$

so that the coefficients in the normalized equation (10) at the terms $(\varrho c_p)^{-1}\sigma E_z^2$ and $(\varrho c_p)^{-1}\Psi$ are equal to unity and the characteristic Prandtl number Pr and the characteristic Reynolds number Re are derived from the normalization constants by the relations:

$$Pr = \frac{c_{p0}\eta_0}{\lambda_0}, \quad Re = \frac{\varrho_0 u_0 L_0}{\eta_0}, \tag{16}$$

where η_0 is an artificially introduced characteristic value of viscosity. The characteristic value of the product $Pr.Re$ which occurs in eq. (10) then is

$$Pr\,Re = \frac{\varrho_0 c_{p0} u_0 L_0}{\lambda_0} = 100. \tag{17}$$

It is of course possible to choose any other set of normalization constants, the above ones being chosen in such a way as to characterize average values for the plasma of a typical arc discharge. The results are dependent on the single

geometric parameter R which enters the set of normalization constants owing to the convenient relation $L_0 = R$.

It is assumed that the functions

$$\sigma = \sigma(T), \quad \lambda = \lambda(T), \quad \varrho = \varrho(Y), \quad c_p = c_p(T), \quad \Psi = \Psi(T) \tag{18}$$

are known.

From the mathematical point of view the equation of heat energy balance is a second-order non-linear partial differential equation of parabolic type. As a method of numerical solution we have chosen the method of lines (see, for example, [3], chap. 14, sec. 6) based on the space discretization of eq. (10) and solving the resulting set of ordinary differential equations by some suitable method. The discretization has been done on an equidistant mesh of N points over the interval $\langle 0, R\rangle$ by the usual method of finite differences. The first and second space derivate of the temperature are calculated by the three-point approximation formulas

$$\left.\frac{\partial T}{\partial r}\right|_i \doteq \frac{T_{i+1} - T_{i-1}}{2h} \tag{19}$$

$$\left.\frac{\partial^2 T}{\partial r^2}\right|_i \doteq \frac{T_{i-1} - 2T_i + T_{i+1}}{h^2}, \tag{20}$$

where $h = R/(N-1)$ is the mesh step. Thus the following set of N first-order ordinary non-linear differential equations is obtained:

$$\left.\frac{\mathrm{d}T}{\mathrm{d}t}\right|_i = \frac{1}{\varrho_i c_{pi}}\left\{\sigma_i E_z^2 + \frac{1}{Pr}\frac{1}{Re}\left[\frac{\lambda_i}{h^2}\left\langle\left(\frac{1}{2(i-1)}+1\right)T_{i+1} - 2T_i - \left(\frac{1}{2(i-1)}-1\right)\right\rangle T_{i-1} + \frac{\lambda_{i+1}-\lambda_{i-1}}{4h^2}(T_{i+1}-T_{i-1})\right] - \Psi_i\right\} \tag{21}$$

$i = 2, 3, \ldots, N-1$

$$\sigma_i \equiv \sigma(T_i), \quad \lambda_i \equiv \lambda(T_i), \quad \varrho_i \equiv \varrho(T_i), \quad c_{pi} \equiv c_p(T_i), \quad \Psi_i \equiv \Psi(T_i) \tag{22}$$

with the boundary conditions

$$T_N(t) = T_R; \tag{23}$$

$$\left.\frac{-3T_i + 4T_{i+1} - T_{i+2}}{2h}\right|_{i=1} = 0 \tag{24}$$

and the initial conditions

$$T_i(0) = T_0(r_i), \qquad i = 1, 2, \ldots, N. \tag{25}$$

This set of equations turned out to be stiff (see, for example, [3], chap. 9, sec.1). This means that all its solutions are damped in time and the ratio of the largest damping time constant to the smallest one is very large. Such set of differential equations must be solved by specialized numerical methods. We have chosen the Gear—Hindmarsh algorithm [10] which is a predictor-corrector method with a variable step ensuring by a special iterative process in the corrector the numerical stability of the solution and the requisite accuracy. The subprograms GEAR [4], GEARB [5] (for sets with a banded Jacobian matrix) and EPISODE [6] were used. The Runge—Kutta method RKF45 [8] proved unsuitable.

Numerical computations have been carried out for nitrogen N_2 under atmospheric pressure $p = 10^5$ Pa. The necessary transport and thermodynamic functions σ, λ, ϱ, c_p, Ψ were available in the table form [7] in the temperature range 500 K—30000 K with the step 500 K. These quantities are plotted in Figs. 1 to 5.

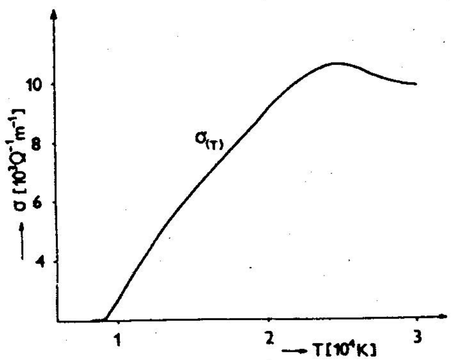

Fig. 1. Electric conductivity of nitrogen vs temperature.

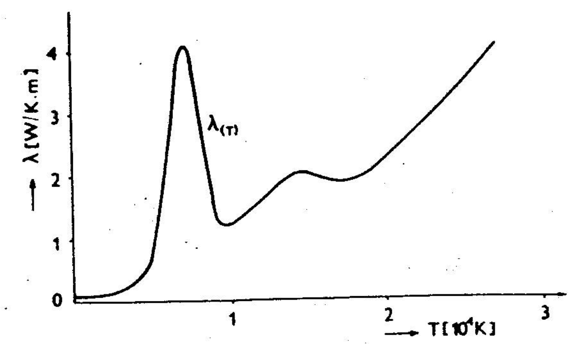

Fig. 2. Thermal conductivity of nitrogen vs temperature.

The interpolation in the tables of transport and thermodynamic functions has been made by means of cubic splines so that the functional values σ, λ, ϱ, c_p, Ψ could

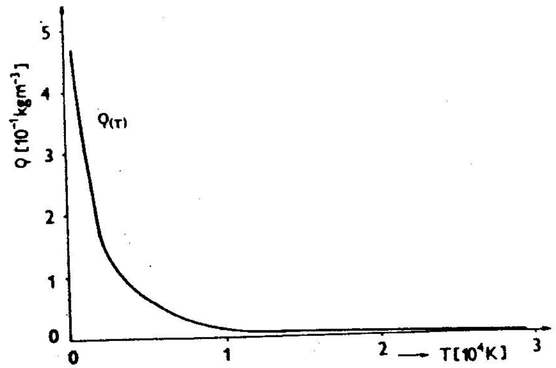

Fig. 3. Mass density of nitrogen vs temperature.

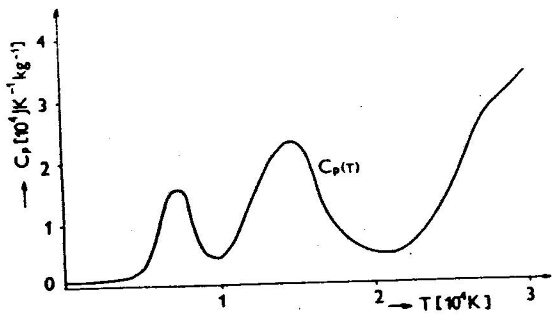

Fig. 4. Specific heat at constant pressure of nitrogen vs temperature.

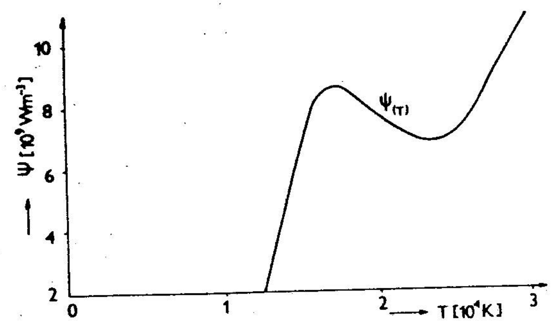

Fig. 5. Radiative energy emitted per unit volume and unit time by nitrogen vs temperature.

be calculated for an arbitrary temperature T. The subprograms SPLINE, SEVAL [8] proved very efficient for this purpose.

The boundary condition at the channel wall has been fixed at $T_R = 500$ K. The initial condition has been chosen is the form

$$T_0(r) = (T_{axis} - T_R)\cos\frac{\pi}{2}t + T_R. \tag{26}$$

IV. RESULTS OF COMPUTATION

The computer model has been thoroughly verified in a series of computational runs. All variants of the integration methods provided by the subprograms GEAR, GEARB and EPISODE have been tried and evaluated from the point of view of accuracy, stability and efficiency. The influence on the accuracy of results of the number of mesh points and of the order of approximation of the difference scheme has also been examined.

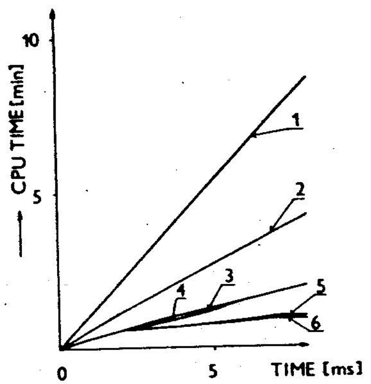

Fig. 6. Computer time vs the physical time of the problem. Curves 1, 3, 5 show the performance of the subprogram GEAR (general Jacobian matrix), curves 2, 4, 6 of the subprogram GEARB (banded or nearly banded Jacobian matrix). Curves 1, 2 — Jacobian matrix approximated by finite difference, 3, 4 — functional iteration, 5, 6 — diagonal approximation of the Jacobian matrix. The prescribed relative error was 10^{-4}.

The best performace has been found with the variants using the diagonal approximation of the Jacobian matrix included in the subprograms GEARB and EPISODE. It was practically ten times faster than the variant using the finite-difference approximation of the Jacobian matrix in the subprogram GEARB. The methods based on the functional iterations were slower. The dependence of the requisite computer time on the physical time for the computer IBM 370/135 is shown in Fig. 6. The differences in the computer stationary state values were always within the bounds given by the prescribed relative error.

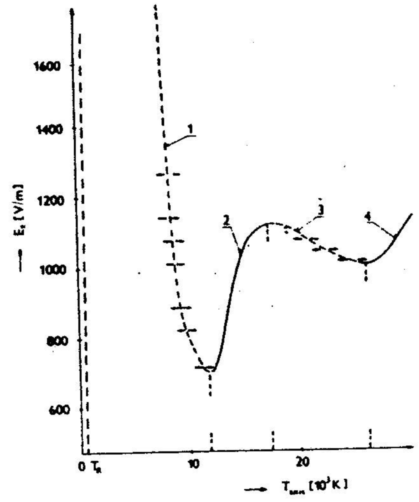

Fig. 7a. E_z vs T_{axis} in stationary state. Curves 1, 3 — unstable branches, 2, 4 — stable branches. The small arrows show the direction of the time evolution of the axial temperature away from the unstable stationary state.

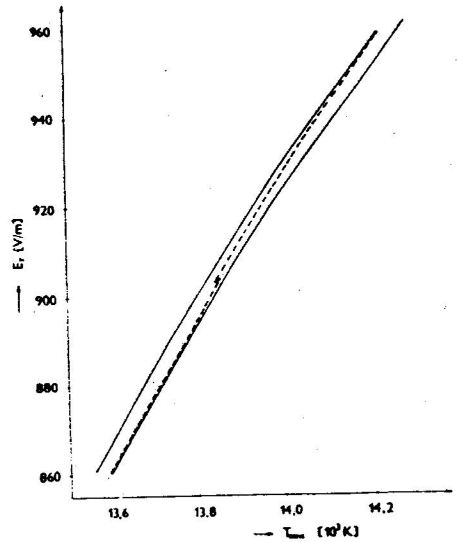

Fig. 7b. E_z vs T_{axis} in stationary state. Detail of the fine structure of the stable branch 2 in Fig. 7a.

The physical results which have been obtained are interesting mainly from the point of view of the discharge stability. Figures 7a and 7b show the dependence of the electric field strength E_z on the temperature T_{axis} at the axis of the channel in the stationary state. There exist three stable and three unstable branches except for the trivial stationary solution $T(r,t) = T_R$ (quenched arc).

The other solutions in the considered range of the electrical field strengths E_z and axial temperatures T_{axis} converge either to the trivial solution (quenched arc) or increase beyond the limits given by the temperature range in the tables of the quantities (18).

It is remarkable that in the temperature interval 13 600 K—14 225 K the dependence E_z vs T_{axis} is threefold. The detail of this dependence is in an enlarged scale presented in Fig. 7b. In Fig. 7a this fine structure is hidden in the width of the line. Whether the stationary state will be achieved on the upper or on the lower stable branch during the evolution depends in this region not only on the axial temperature but also on the form of the initial condition. In all the other temperature regions the resulting stationary state is, in wide intervals, independent of the shape of the initial condition.

Fig. 8 illustrates the dependence of the electric field strength E_z on the total current I which flows along the channel (current-voltage characteristic). The branches which are shown correspond to the stable branches in the preceding $E_z(T_{axis})$ diagram. The current jumps correspond to the unstable branches in the $E_z(T_{axis})$ diagram. The first current jump is caused by the dissociation of the N_2 molecules and is accompanied by an abrupt change of the stationary radial temperature profile (cf. Fig. 9 and Fig. 10). The second current jump is obviously caused by the decrease of Ψ (radiative energy emitted per unit volume and unit time) in the temperature region from 17 500 K to 23 500 K and is not accompanied by any qualitative change of the stationary temperature profile.

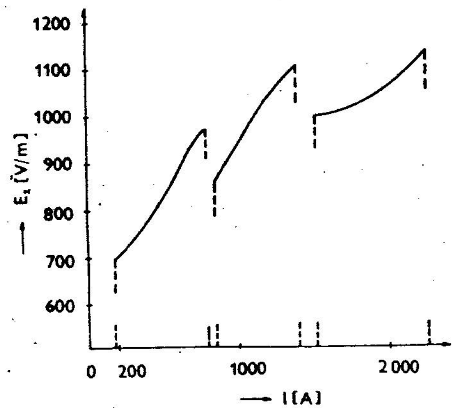

Fig. 8. Current-voltage characteristic.

Fig. 9 and Fig. 10 show the typical stationary temperature profiles — the dependence of temperature on the non-dimensional radius r. On both graphs the curves No. 1 mark the temperature profile at the time instant $t = 0$ (the initial curves No. 1 mark the temperature profile at the time instant condition), the curves No. 2 and No. 3 indicate the stationary temperature profiles which have been solved on a mesh of 11 and 21 points along the radius, respectively. The stationary temperature profile shown in Fig. 9 exhibits the formation of a high temperature core and is typical of the lowest stable branch of the current-voltage characteristic. The temperature profile shown in Fig. 10 is typical of the two higher stable branches.

Fig. 11 demonstrates the current density profiles. The individual curves 1, 2, 3, 4 correspond to stationary states with various values of T_{axis} and E_z. For these

profiles a steep decrease of the current density towards the wall of the channel is characteristic.

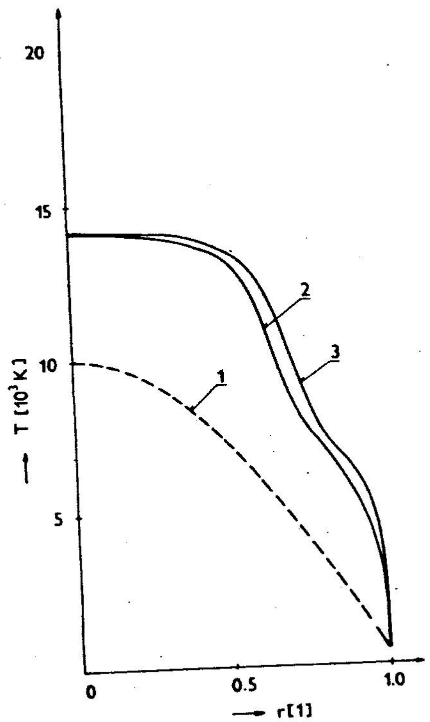

Fig. 9. Radial temperature profiles. Curve 1 — initial condition; 2, 3 — stationary temperature profiles (T_{axis} = 14 120 K, E_z = 949 V/m, $N = 11$ (curve 2), $N = 21$ (curve 3)).

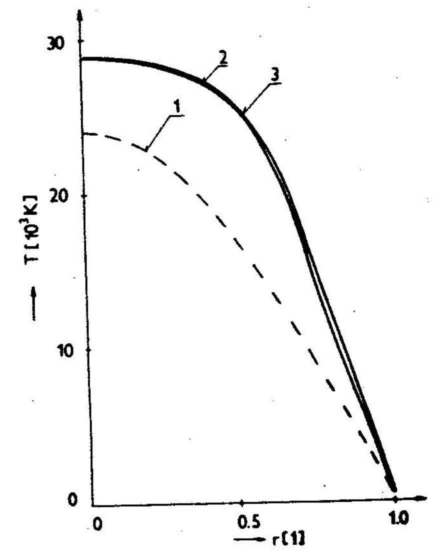

Fig. 10. Radial temperature profiles. Curve 1 — initial condition; 2, 3 — stationary temperature profiles (T_{axis} = 28 852 K, E_z = 1 075 V/m, $N = 11$ (curve 2), $N = 21$ (curve 3)).

The calculated temperature profiles can be compared with the results published in [9]. In Fig. 12 a temperature profile from [9] is reproduced corresponding to T_{axis} = 11 650 K, E_z = 631 V/m. According to Fig. 7a there corresponds to this axial temperature an unstable stationary state. We have therefore compared the closest stable stationary profile corresponding to T_{axis} = 12 356 K (minimum E_z on branch 2). Although the material and thermodynamic functions for nitrogen utilized in [9] differ to a large extent from those in [7], which were utilized in

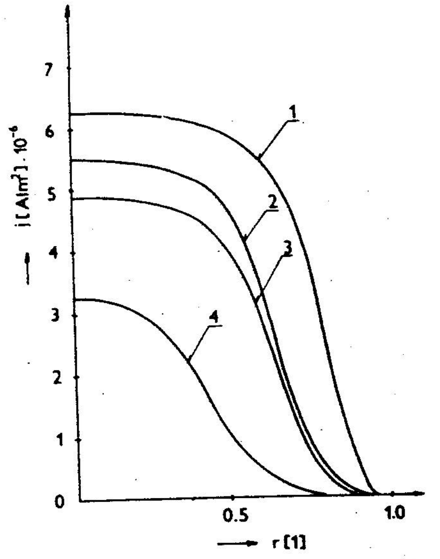

Fig. 11. Radial current density profiles. Curve 1 — T_{axis} = 14 718 K, E_z = 10 12 V/m; 2 — T_{axis} = 14 120 K, E_z = 949 V/m; 3 — T_{axis} = 13 691 K, E_z = 885 V/m, 4 — T_{axis} = 12 457 K, E_z = 705 V/m.

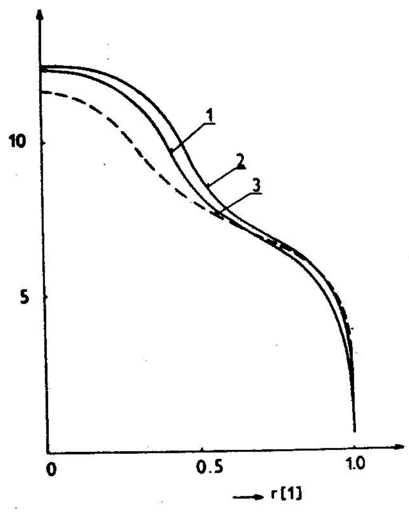

Fig. 12. Radial temperature profiles. Curves 1, 2 — calculated stationary temperature profiles (T_{axis} = 12 356 K, E_z = 697 V/m, N = 11 (curve 1), N = 21 (curve 2)), curve 3 — a temperature profile published in [9] (T_{axis} = 11 650 K, E_z = 631 V/m).

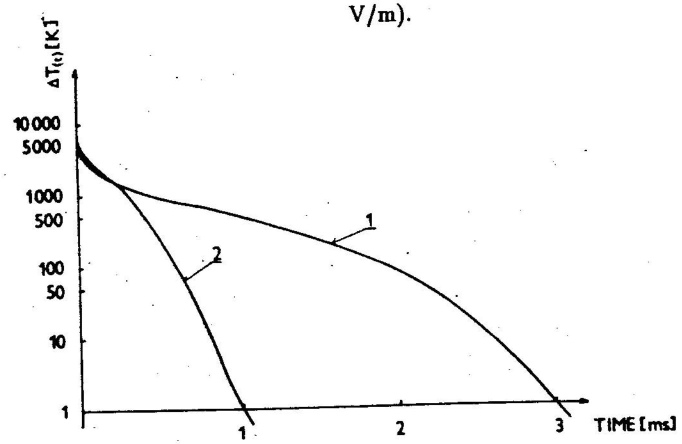

Fig. 13. The evolution of the axial temperature. $\Delta T(t) = T_{axis}(\infty) - T_{axis}(t)$. Curve 1 — the approach to the stationary value $T_{axis}(\infty)$ = 14 120 K from the value $T_{axis}(0)$ = 10 000 K, for E_z = 949 V/m, 2 — the value $T_{axis}(\infty)$ = 28 852 K, $T_{axis}(0)$ = 23 000 K, E_z = 1 075 V/m. The corresponding initial conditions and stationary temperature profiles are in Fig. 9 and 10, respectively. The 1 K level approximately corresponds to the magnitude of the rounding noise of the time integration.

our computations, it is apparent from Fig. 12 that the agreement of the results is relatively good.

As an example of the non-stationary behaviour of the electric arc discharge we present in Fig. 13 two time dependences of the axial temperature illustrating the transient phenomenon during the approach to equilibrium. It is apparent that the relaxation times are of the order of milliseconds and that at the beginning the plot is significantly different from the exponential. The exponential behaviour is approached only in the close vicinity of the stationary state.

V. CONCLUSION

We hope that we have demonstrated the usefulness of the non-stationary model of the discharge channel of an electric arc gas heater.

The experience with the present simple model indicates that it will be possible to employ the same concept as a basis for the construction of a two-dimensional model. We have proved the realizability of the non-stationary model, the applicability of the Gear—Hindmarsh algorithm for the time integration of the resulting set of differential equations (regardless of other possible methods of the space discretization) and the sufficient accuracy of the formation of the material and thermodynamic function by means of a simple cubic spline interpolation.

We intend to extend the present computer model by the model of an external electrical circuit with a source of electromotive force and resistance and to study certain transient phenomena, like the ignition process. The solutions for other working gases (hydrogen, argon, water vapour) are also being considered.

ACKNOWLEDGEMENTS

The authors are grateful to Dr. Rudolf Hajossý of the Department of Experimental Physics of the Faculty of Mathematics and Physics of the Comenius University in Bratislava for his helpful comments.

REFERENCES

[1] Zarudi, M. E.: Těplofizika vysokich těmperatur *1(1968)*, 35.
[2] Zhukov, M. F., et al.: *Prikladnaia dinamika termitsheskoi plazmy.* Nauka, Novosibirsk 1975.
[3] Hall, G., Watt, J. M.: *Modern Numerical Methods for Ordinary Differential Equations.* Clarendon Press, Oxford 1976.
[4] Hindmarsh, A. C.: UCID-30 001 Rev. 3, Livermore Dec. 1974.
[5] Hindmarsh, A. C.: UCID-30 059 Rev. 1, Livermore March 1975.

[6] Hindmarsh, A. C., Byrne, G. D.: UCID-30 112, Livermore May 1975.
[7] Yos, J. M.: *Transport Properties of Nitrogen, Hydrogen, Oxygen and Air.* AVCD Corp., Wilmington (Mass) 1963.
[8] Forsythe, G. E. et al.: *Computer Methods for Mathematical Computations.* Prentice-Hall, New Jersey 1977.
[9] Schmitz, G. et al.: Zeitschrift für Physik *173* (1963), 552.
[10] Gear, C. W.: *Numerical Initial Value Problems in Ordinary Differential Equations.* Englewood Cliffs, New Jersey 1971.

Received February 22nd, 1989
Accepted for Publication April 3rd, 1990

НЕСТАЦИОНАРНАЯ ЧИСЛЕННАЯ МОДЕЛЬ АСИМПТОТИЧЕСКОЙ ОБЛАСТИ ПЛАЗМОТРОНА

В работе приведен для численного решения нестационарного уравнения баланса энергии в асимптотической области плазмотрона с аксиальным подводом газа, который делает возможным различение устойчивых и неустойчивых решений в детальное рассмотрение переходного явления при установлении стационарного состояния.